

# *Monitoring of the lung fluid movement and estimation of lung area using Electrical Impedance Tomography: A Simulation Study*

Deborshi Chakraborty

Dept. of Instrumentation Science  
Jadavpur University, Kolkata: 700 032, India  
E-mail: dchphy123@gmail.com

Madhurima Chattopadhyay

Dept. of Applied Electronics and Instrumentation Engg.  
Heritage Institute of Technology, Kolkata: 700 107, India  
E-mail: madhurima02@gmail.com

**Abstract**— Patients suffering from the acute respiratory distress syndrome (ARDS) requires thoracic electrical impedance tomography (EIT) for the monitoring their conditions ranging from dynamic shifting of body fluids to lung aeration right at the bedside. More objectively, EIT-derived numeric parameters would help the physician to evaluate the state of the lung. Thus, here we have performed a Finite Element Method based simulation study for monitoring the condition of lungs and heart of ARDS patients. Therefore, a finite element method (FEM)-model of a human thorax in 3 dimensional platform of FEM Multiphysics software is created and is tested with new ventilation indices regarding their ability to quantitatively describe structural changes in the lung due to the gravitationally dependent lung collapse. Additionally, analysis is made to find the electrode pairs capable of separating the lung and heart activity when a particular amount of constant current is injected through them are also carried out. Finally, a real time of the EIT system using 16 Ag-AgCl electrodes were developed for real time imaging of the human thorax. The data were collected using the adjacent current injection technique and are plotted using FEM Multiphysics software. The reconstructed FEM images using the forward solver of EIT shows the approximate area of the thorax (lungs, heart etc.) under observation.

**Keywords**— *Electrical Impedance Tomography (EIT); Finite Element Method (FEM); Acute Respiratory Distress Syndrome (ARDS); heart activity; lungs activity.*

## I. INTRODUCTION

The estimation of the spatial conductivity distribution in a thorax cross section is carried out by thoracic electrical impedance tomography (EIT) as it is a non-invasive technique[1-4]. In this procedure, the electrodes are equidistantly attached to the patient's skin around the thorax. During a measurement, adjacent electrodes are fed with a small alternating currents and the potentials at the remaining electrodes are measured (i.e., adjacent drive/adjacent receive). Then, reconstructed images with this data visualize the change in conductivity of the specific area of interest[5]. In recent years, EIT is use to monitor a variety of clinical problems such as respiratory failure, cardiac volume changes, gastric emptying, and head imaging [6]. In spite of low spatial resolution (about one tenth of the thorax diameter), but due to its non-invasiveness and high temporal resolution it seems to

be particularly useful for the bedside monitoring of patients suffering from the acute respiratory distress syndrome (ARDS) [7]. ARDS is a life-threatening state of the lung characterized by atelectasis (i.e., lung collapse) and pulmonary edema (i.e., water in the lung) and thus, variations of the conductivity distribution in the thorax. ARDS patients have to be mechanically ventilated with higher oxygen concentrations and changing pressure levels resulting in dynamic shifts of body fluids and lung aeration. For visualizing those shifts, EIT is well suited in providing an instantaneous feedback to the medical staff [8, 9]. In order to achieve maximum benefit, further investigations is to be carried out to process the fast sequence of EIT images (up to 50 images/s) and also the way out for the extraction and quantification of the underlying physiological information. The attending physician should be able to immediately recognize ventilation changes in the lung resulting from, e.g., new ventilator settings. EIT-derived numeric parameters could be able to evaluate the objective more precisely in comparison with the visual observations of the EIT images (subtle changes are simply hard to detect). Additionally, EIT-based trend can analysis for different kinds of diseases with the help of numeric parameters. Therefore, we first created a 2D finite element model of the human thorax and divided the lung into three coronal layers. Then, we altered the fluid contents of the dorsal layers close to the back in order to simulate lung collapse of increasing severity. Then the thorax model from the 2D plate were transformed to the 3D plane for the analysis. After reconstruction, we looked at different methods to quantify the given ventilation changes and compared them with the actual modifications made in the thorax model. From this EIT based reconstructed images an approximate determination of the lung area is obtained.

Finally, as EIT seems also to be capable of distinguishing between heart and lung related changes of the conductivity in the thorax [10], we examined which current-injection and voltage measurement electrode pairs are best suited for a proper separation between lung and heart activity. Hence, we calculated the average current density for the different tissues and compared them based on the position of the current injection.

## II. METHODS

### A. Modeling

An adequate geometric model of the human thorax is designed with realistic values of the electrical properties of biological tissue for the proper assessment of lung collapse. Thus, a correct geometric dimension of the model (shown in Fig. 1(a)) from real CT images of a human male. During the mesh generation, necessary simplifications and conditions are made were similar to the ones described in [11]. The resulting mesh consisted of 454847 first-order triangular elements are created with FEM based Multiphysics software. In total, five different types of tissue were being modeled with electrical properties taken from the literature: muscle, heart, bones (spinal column, ribs, and sternum), fat, and lung; cf. Table I. The currents of 10 mA @200 kHz (as frequencies between 20 and 200 kHz are widely used for thoracic single-frequency EIT) are injected across the electrode pair. In order to simulate patient breathing, conductivity and relative permittivity of the lung were varied between deflated and inflated lung as given in [12]. Visceral movements (i.e., geometric changes) during a breath cycle are not considered as it has been reported to have a rather low influence for state-differential reconstruction algorithms [13].

Patients suffering from acute respiratory failure are usually treated in supine position. Due to the weight of its upper parts, the lung tends to collapse in the lower parts first (commonly termed as gravitationally dependent collapse). Therefore, we divided the lung into three coronal layers and modeled different amounts of lung collapse by subsequently replacing the bottommost layers with collapsed lung tissue [Fig. 1(a)] without any breathing activity. The electrical properties of the collapsed areas (0.6 S/m, 1000) were assumed to be a mixture of deflated lung tissue and well-conducting body fluid [14].

This straightforward simplification should be sufficient, as mainly the missing ventilation of the collapsed lung tissue will influence the reconstructed images of conductivity change. Fig. 1 provides the details overview of the electrode placement and numbering of adjacent electrode pairs. For the simulation of the heart activity, variation of its electrical properties between "normal" heart and blood-filled heart (a mixture of blood and heart properties: 0.45 S/m, 11 000) were considered. As before, to obtain qualitative character, the geometric changes during a breath cycle are omitted.

TABLE I. ELECTRICAL PROPERTIES OF THE MODELED TISSUES BETWEEN 20 - 200 KHZ [12].

Tissue	Conductivity (S/m)	Relative permittivity
Lung* (deflated)	0.26197	8531.40
Lung *(inflated)	0.10265	4272.50
Heart*	0.19543	16982.00
Bone* (cortial)	0.02064	264.19
Fat*	0.02424	172.42
Muscle*	0.35182	10094.00
Body Fluid	1.50000	98.56

Tissue	Conductivity (S/m)	Relative permittivity
Blood	0.70080	5197.70

(Asterisk-Marked (\*) properties were used for the simulation of the reference state)

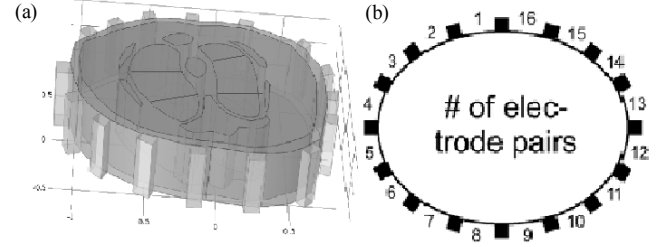


Fig. 1. (a) Electrode placement and (b) numbering of electrode pairs

### B. Mathematical Model

For a known conductivity, a relationship can be established between the electrical conductivity ( $\sigma$ ) and spatial potential ( $\Phi$ ), to calculate the nodal potential [17]. Electro-dynamics of EIT is governed by a nonlinear partial differential equation, called the Governing Equation [17] of EIT, is given by,

$$\nabla \cdot \sigma \nabla \Phi = 0 \quad (1)$$

The potential field inside of the conductor having no internal electrical sources or sinks, must satisfy the equation (1). To solve this equation, the following boundary conditions are to be known

a) *Dirichlet Boundary Condition:*

$$\Phi = \Phi_i \quad (2)$$

Where,  $i = 1 \dots N$ , are the measured potentials on the electrodes.

b) *Neumann Boundary Condition:*

$$\int_{\partial\Omega} \sigma \frac{\partial \Phi}{\partial \eta} = \begin{cases} +I \\ -I \\ 0 \end{cases} \quad (3)$$

Here, +I is for source electrode, -I is for sink electrode and 0 otherwise.  $\partial\Phi$  is the boundary and  $\eta$  is the outward normal vector to the electrode surface. In this paper forward problem solver algorithm is used. The description of this problem is discussed below.

c) *Forward Problem*

A relation can be obtained between the voltage measurements made on the boundary ( $\partial\Omega$ ) and the domain conductivity can be found [12, 13] as,

$$\Phi = K \sigma \quad (4)$$

Where  $\sigma$  is a vector of conductivity values,  $\Phi$  is the vector of voltage measurements and K is the transformation matrix relating  $\Phi$  to  $\sigma$ .

If  $K$  and  $\sigma$  are known, equation (1) can be solved numerically using FEM to calculate the nodal potentials of the domain for the known conductivity ( $\sigma$ ). It is known as the “forward problem”.

Thus, for a known value of a constant current, the nodal potentials within the phantom area are computed using the forward solver problem of EIT [15, 17]. The value of the conductivity and permittivity of the blood, body fluids etc. of the designed FEM model are obtained from Luepschen et al. [20].

### C. Field Simulation

The FEM Multiphysics software is used to simulate the models. Simulations are conducted similar to the measuring procedure of the EIT system. For each physiological state of the lung, 16 simulations are to be carried out to account for all current-injection positions while determining the voltages between the remaining 13 electrode pairs. Hence, voltages distributions is determined for each state of the lung (shown in Fig. 2).

### D. Image Reconstruction and Processing

State-differential EIT images were reconstructed from the simulated 208 voltages using the forward algorithm [17] and the boundary conditions as discussed in section B. The reconstructed images represent the conductivity changes based on either the breathing or the heartbeat activity. In order to quantify dorsoventral as well as lateral shifts of the ventilation distributions resulting from different amounts of lung collapse are studied [18].

## III. RESULTS AND DISCUSSIONS

### A. Determination of Heart Activity

The amount of current through the different tissues is obviously influenced by the position of the current-injection electrode pair. Electrode pair #5 will lead to a greater amount of current flowing through the (right) lung, whereas injection through electrode pair #16 maximizes the current flow in the heart it can easily be visualize from the plot of the ratio of the current density of heart to that of the lungs as shown in Fig. 3.

The corresponding current density images of the FEM simulations are provided in Fig. 2. The qualitative results for the best electrode pairs to measure the heart activity were additionally backed up by looking at the voltage changes at the boundary. Especially, when using the identified optimal current-injection electrodes as receiver electrodes (e.g., current-injection pair: #16, receive pair: #8), SNR was maximized (here, the lung activity is regarded as “noise”).

From the Fig. 3 it is seen that depending on the position of the current-injection electrode pair, the amount of current through heart and lung varies. For the detection of the heart activity,

electrode pairs #1, #8, #9, #15, and #16 provide the best chances for the observation.

### 3.2. Determination Of Lung Collapse And Lung Area

From the Fig. 4 it is seen that the different amount of collapsed lung area which is determined by forward solver algorithm.

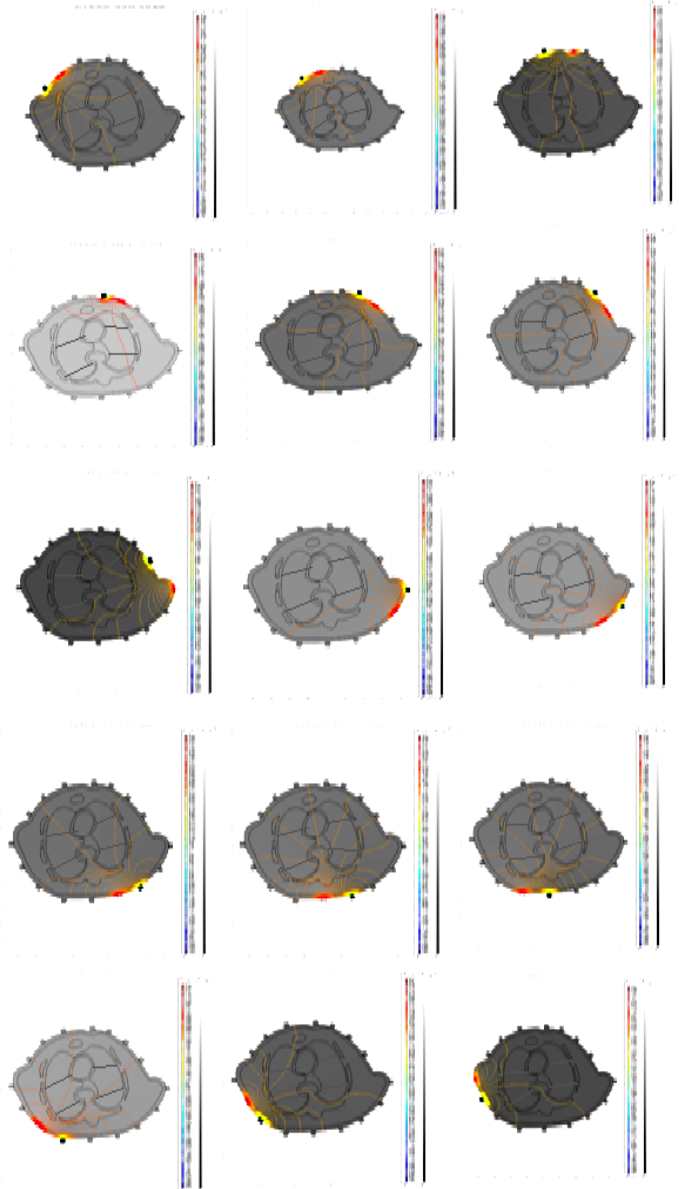


Fig. 2. Current density distribution and potential isolines plots from the FEM based simulation study for different current-injection positions.

The voltage distribution plots as of the lungs in Fig. 4 shows that the collapse of different layers of the lungs starting from the lowermost part.

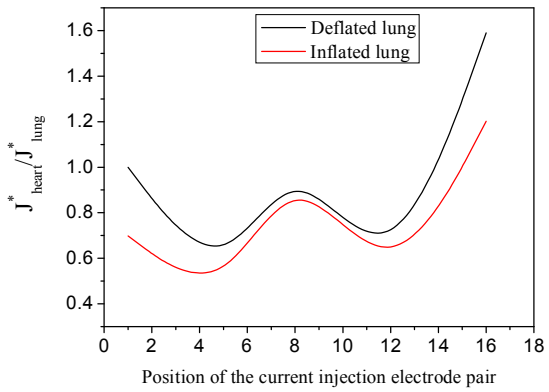


Fig. 3. Plot of current densities of heart and lungs  $J^*_{heart}$  and  $J^*_{lung}$  vs. the position of the current injection electrode pair

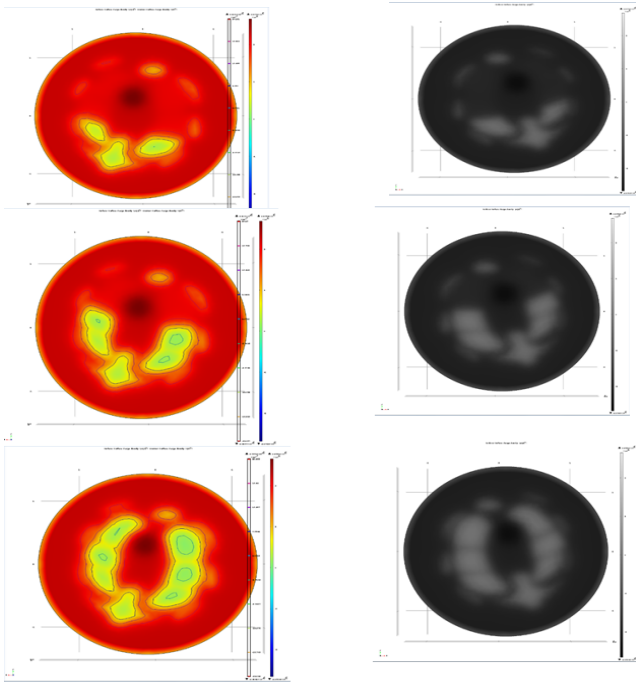


Fig. 4. Reconstructed differential EIT images for different amounts of collapsed lung with forward solver algorithm

From these figures approximate determination of the lung area can also be estimated, which can provide an overview condition of the lungs to the physician.

### B. Real time studies

For the real time analysis, a 16 electrodes array of Ag-AgCl are developed for imaging of the human thorax. The electrodes are been circular with an radius of about 1cm. The electrodes are placed equidistantly with spacing of 3cm. This

spacing is adjustable as per the size of the thorax of the objective.

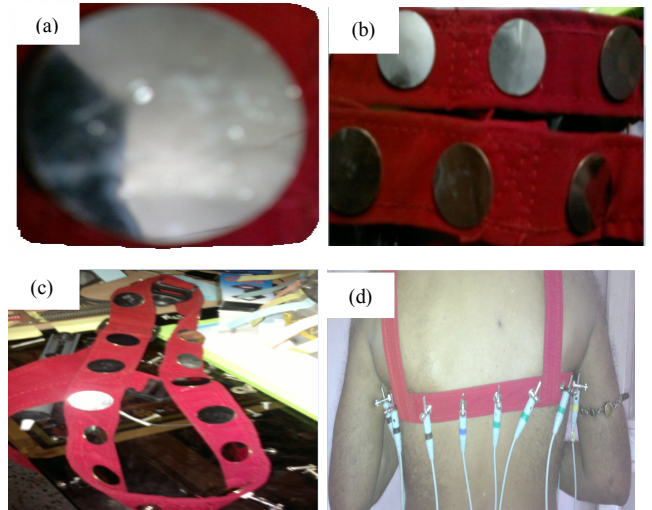


Fig. 5. Photograph of (a) Single Ag-AgCl electrode, (b),(c) showing the arrangement of the 16 electrodes in the array belt and (d) objective wearing the belt for imaging of the thorax

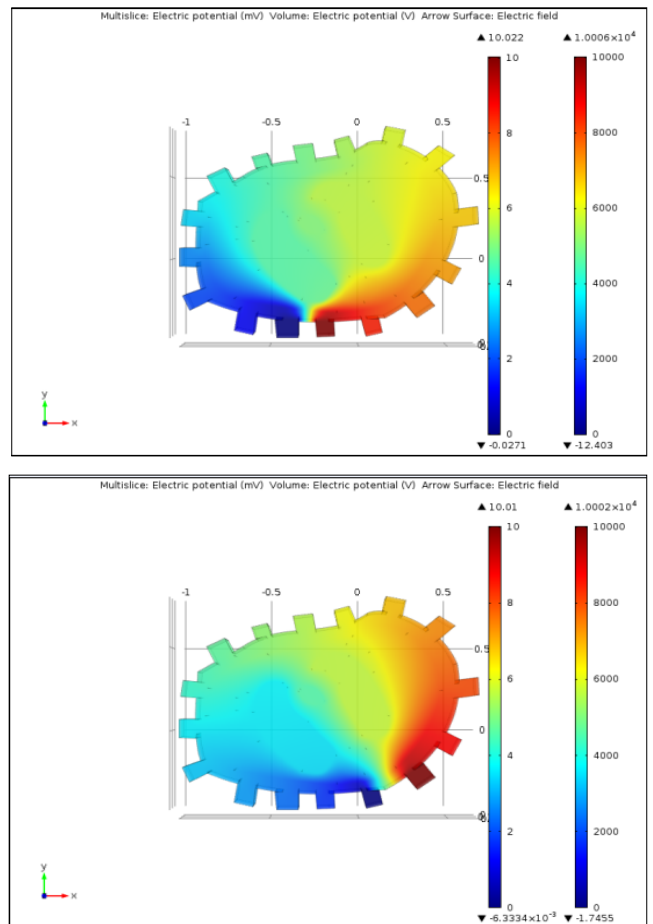


Fig. 6. Voltage density plots of the data obtained from the real time imaging of the thorax using adjacent protocol type current (10 mA, 20-200 KHz) injection pattern .

The real time data using the electrode array were obtained along a single plane of the human thorax. A current of 10 mA, 20-200 KHz were injected across the electrodes using adjacent current injection protocol. The boundaries were obtained manually and were recorded and fed into FEM based multiphysics software to obtain the voltage density plots shown in the Fig. 6. The figure shows that the reconstructed images using forward solver of EIT of human thorax in a single plane is obtained successfully. From the plots an approximate area coverage of the lungs as well as the human thorax is estimated for analysis.

#### IV. CONCLUSIONS

During EIT measurements, studies on the electromagnetic field distribution in the human thorax are important to understand because it provides an estimated idea relating to the varying current paths. This knowledge is very much vital to understand the pathological changes obtained from the EIT-based observations.

The electrode pairs #1, #8, #9, #15, and #16 provide the best SNR for the detection of the heart activity. The influence of the lung activity is minimized while considering these pairs of electrodes. In considering the structural changes due to the breathing and the heart beat would give more precise understanding of the occurring reconstruction artifacts.

Finally in a future, a complete analysis of the human thorax using real time implemented system of 16 Ag-AgCl electrodes is to be performed to be correlated with the simulated results.

#### ACKNOWLEDGMENT

The author Deborshi Chakraborty like to acknowledge Department of Science and Technology, Govt. of India, for providing financial assistantship as INSPIRE Fellowship.

#### REFERENCES

- [1] Mohd Tahir Erwati, & Nagi Farrukh, "Applications of electrical impedance tomography for imaging in biomedical and material technology", Proc. of 2009 IEEE Students Conference on research and development (SCoReD 2009), 16-18 Nov '09, UPM Serdang, Malaysia.
- [2] Sarwan Kumar, Sneha Anand & Amit Sengupta, "Impedance based image reconstruction of the field distribution inside the closed phantom using finite element method", (IJCNIS) International journal of computer and network security. Vol. 2, No 7, July 2010.
- [3] Y. Zou & Z. Guo, "A review of electrical impedance techniques for breast cancer detection" Elsevier Medical Engineering and Physics 25 / (2003).
- [4] Jianjun Zhang, Weili Yan, Guizhi Xu & Quanming Zhao, "A New Algorithm to Reconstruct EIT Images; Node Back Projection Algorithm", Proceedings of the 20th Annual International conference of IEEE EMBS. Cite Internationale, Lyon, France August 23-26, 2007.
- [5] John G. Webster, "Medical Instrumentation Application and Design", third edition, Wiley India, 2007,.
- [6] B. H. Brown, "Electrical impedance tomography (EIT): A review," J.Med. Eng. Technol., vol. 27, pp. 97-108, 2003.
- [7] H. Luepschen, T. Meier, M. Grossherr, T. Leibecke, J. Karsten, and S. Leonhardt, "Protective ventilation using electrical impedance tomography," Physiol. Meas., vol. 28, pp. S247-S260, 2007.
- [8] J. A. Victorino et al., "Imbalances in regional lung ventilation—A validation study on electrical impedance tomography," Am. J. Respir. Crit. Care Med., vol. 169, pp. 791-800, 2004.
- [9] T. Meier, H. Luepschen, J. Karsten, T. Leibecke, M. Grossherr, H. Gehring, and S. Leonhardt, "Assessment of regional lung recruitment and derecruitment during a PEEP trial based on electrical impedance tomography," Intensive Care Med., July 25, 2007, Epub ahead of print.
- [10] H. Smith et al., "Electrical impedance tomography to measure pulmonary perfusion: Is the reproducibility high enough for clinical practice?," Am. J. Respir. Crit. Care Med., vol. 24, no. 2, pp. 491-9, 2003.
- [11] O. A. Mohammed and F. G. Uler, "Detailed 2-D and 3-D finite element modeling of the human body for the evaluation of defibrillation fields," IEEE Trans. Magn., vol. 29, no. 2, pp. 1403-6, Mar. 1993.
- [12] Institute for Applied Physics, Italian National Research Council, "Dielectric properties of body tissue," Jun. 2007 [Online]. Available: <http://niremf.ifac.cnr.it/tissprop>
- [13] A. Adler, R. Guardo, and Y. Berthiaume, "Impedance imaging of lung ventilation: Do we need to account for chest expansion?," IEEE Trans. Biomed. Eng., vol. 43, pp. 414-420, 1996
- [14] Alistair Boyle, Andy Adler, and William R. B. Lionheart; "Shape Deformation in Two-Dimensional Electrical Impedance Tomography"; IEEE Transactions on Medical Imaging, Vol. 31, No. 12, December 2012.
- [15] P. Ghaderi Daneshmand, R. Jafari "A 3D hybrid BE-FE solution to the forward problem of electrical impedance tomography", Engineering Analysis with Boundary Elements, Volume 37, Issue 4, 2013, pp.757-764.
- [16] D. K. Anderson, R. C. Tozer, I. L. Freeston, "Analytic solution of the forward problem for induced current electrical impedance tomography systems", IEE Proc.-Sci. Mens. Technol., Vol. 142, No. 6, November 1995.
- [17] Tushar kanti Bera, J. Nagaraju; "A FEM-Based Forward Solver for Studying the Forward Problem of Electrical Impedance Tomography (EIT) with A Practical Biological Phantom"; Proceeding of 2009 IEEE International Advance Computing Conference (IACC 2009), 6-7 March, 2009, Patiala, India.
- [18] Bushberg; J. T., Seibert; J. A., Leidholdt Jr.; E. M., Boone; John M., "The Essential Physics of Medical Imaging", 2nd Edition, Lippincott Williams & Wilkins, ISBN-10: 0683301187.
- [19] Huanli Wu, Guizhi Xu, Hongli Yu, Shuai Zhang, Ying Li, Shuo Yang and Weili Yan "Three Dimensional Electrical Impedance Tomography in Thorax Complete Model" 30th Annual International IEEE EMBS Conference Vancouver, British Columbia, Canada, August 20-24, 2008 978-1-4244-1815-2/08, IEEE.
- [20] Henning Luepschen et al., "Modeling of Fluid Shifts in Human Thorax for Electrical Impedance Tomography", IEEE Transactions On Magnetics, Vol. 44. No. 6. June 2008.